



## **INFLUENCE OF CHEMICAL COMPOSITION OF STEEL ST3SP ON THE QUALITY OF HOT-ROLLED SHEETS**

**S. A. MASHEKOV, N. K. SMAGULOVA, A. S. MASHEKOVA\* and  
L. A. KURMANGALIEVA**

Institute of Industrial Engineering, Kazakh National Technical University named after K.I. Satpayev,  
ALMATY, REPUBLIC OF KAZAKHSTAN

### **ABSTRACT**

The overall assessment of the influence of chemical composition and structure of sheet ST3SP steel samples on quality of the sheets, rolled by the existing technology on a continuous wide strip mill 1700 was run. The study shows that the control of the hardness of hot rolled strip by changing its chemical composition is only possible through the establishment of a sufficiently accurate content of carbon, manganese and silicon, as well as strictly observe the temperature of rolling, cooling and coiling on the run-out table.

**Key words:** Chemical composition, Steel ST3SP, Hot-rolled sheet.

### **INTRODUCTION**

It is known that the structure of producing hot-rolled metal and its mechanical properties directly depend on its chemical composition, the temperature conditions of rolling and coiling, as well as cooling modes of the strip on the outlet (Table 1). Different microstructure of rolled strip is obtained depending on the rate of cooling (heat removal intensity), hence mechanical properties of the rolled can be modified by varying cooling modes over a fairly wide range.

Higher strength properties of the rolled metal are achieved by increasing the cooling rate under otherwise equal conditions, whereas there is a reduction of its plastic properties<sup>1</sup>. However, it should be noted that the layer of thermohardening metal is formed on the surface of the strip at very high cooling rate. The heterogeneity of the microstructure along the strip thickness, obtained at high cooling rates, increased hardness, and "fragility" of thermohardening surface, all of this together leads to a mismatch of obtained mechanical properties of the hot-rolled with the requirements of the standards, hence defective products

---

\* Author for correspondence; E-mail: aigerim.mashekova@nu.edu.kz

can be produced.

According to the "iron -cementite" phase diagram<sup>2</sup> studied ST3SP steel has a ferrite-pearlite structure at normal temperature. Since the ferrite contains a very small percent of carbon, pearlite is the main carrier of carbon in the steel ST3SP. Therefore, the enlargement of the mass fraction of carbon in the steel leads to a mass fraction increase of the cementite phase in the pearlite, which leads to increased hardness and strength, reduction in ductility and impact toughness.

A number of impurities of Mn, Si, S, P, etc. present in addition to the principal carbon steel components (iron and carbon)<sup>2</sup>. The presence of various impurities is explained by the different underlying causes. Mn and Si in tenths of a percent proceed in the steel during deoxidation; S and P, in hundredths of a percent remain in the steel because of the difficulty of their complete removal; Cr and Ni transferred in the steel from a charge material comprising alloyed metal and allowed no more than 0.3% each. These impurities can form oxides, carbides, intermetallic compounds.

Phases in carbon steels are spaced in a certain way in their volume, forming a particular structure depending on the mass fraction of carbon or impurities. Thus, studies of the chemical composition influence resulting from the cooling phase, the temperature regimes of rolling and coiling as well as cooling modes have a great influence on the quality of the hot-rolled steel.

The aim of this work was a comparative study of the influence of the chemical composition and structure of ST3SP steel sheets on the quality of the sheets, rolled by the existing technology on a continuous wide strip mill 1700.

## **EXPERIMENTAL**

### **Materials and methodology of the experiment**

Samples of ST3SP steel are strips with a length of 500 mm and with a cross section of 4 × 200 mm, cut from a sheet in a position of furnishing by electric spark cutting. The samples were subjected to a mechanical polishing using a polishing paste and subsequent cleaning in organic solvents.

Metallographic analysis was carried out on an optical microscope Axiovert-200 MAT at 200 X, 500 X and 1000 X magnifications. Image processing was carried out by the program Video Test "Metal 1.0", as well as using an energy dispersive spectrometer JNCA Energy (UK), located on the electron probe microanalyzer JEOL at an accelerating voltage

of 25 kW. The range of JEOL instrument magnification is from 40 to 40,000 power. The principle of microanalyzer operation is a high-energy (25 KeV) narrow (1  $\mu\text{m}$ ) ray of electrons is directed onto the sample, where it is set in the raster pattern (frame) by scanning the sample, simultaneously registering secondary electrons emitted by the sample. The resulting picture is very similar to the optical images, but due to the fact that the electron beam is very thin ( $\approx 1\text{-}2\ \mu\text{m}$ ), the depth of focus is much higher than optical images and using magnification is also significantly higher, respectively, it is allowed to distinguish smaller structural components of the sample.

Quantitative analysis of the defective substructure parameters and phase analysis were performed by standard methods<sup>2</sup>. Polished sections for metallographic examination were prepared by the traditional method on grinding and polishing circles. Concentrated solution of acid nitric in ethanol was used for etching the samples. Phases relationship of the sample was calculated by video test- Metal 1.0 software, as a result phases diagrams distribution at different temperatures were obtained.

The chemical composition of the studied steel was determined by the MFS system. The study is based on the method of emission spectral analysis, which uses the dependence of intensity of the spectral lines from the mass fractions of the elements in the sample.

The samples for tensile test were cut from steel rolled by the existing technology. Produced samples were tested in tension at room temperature on a universal testing machine with a force of 100 Kn till the destruction (Fig. 1). After the test the mechanical properties were determined by using graphical and analytical methods in a way of dividing the efforts of the destruction of the cross sectional area of the sample to failure<sup>2</sup>.

## RESULTS AND DISCUSSION

To investigate the influence of the chemical composition and structure on the quality of the hot-rolled strip steel ST3SP, rolled by the existing technology on the uninterrupted broad band mill 1700, the mechanical properties of the sheet samples were studied.

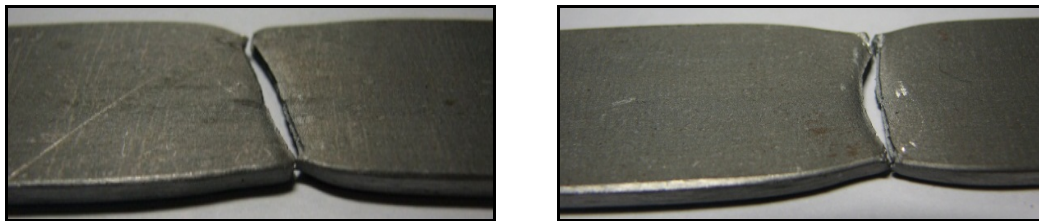


**Fig. 1: A general view of the samples after stretching**

To carry out the above mentioned study a number of samples were cut from sheets for mechanical testing and microstructural analysis. The samples were cut from sheets with dimensions of  $4 \times 880$  mm, which were rolled by the existing technology from different heats slabs. The chemical composition of the steel is shown in Table 1. Dimensions of the samples for mechanical testing before and after the test (Fig. 1) are shown in Table 2. The influence of chemical composition on the mechanical properties of the sheets was examined by regression analysis. As a result, the equations of dependence on tensile strength and yield strength of the ladle sheets of carbon, manganese and silicon were gained.

**Table 1: Chemical composition of shapes rolled from different batches of slabs**

S. No.	Rolling end T (°C)	Coiling T (°C)	C	Si	Mn	S	P	Cr	Ni	Cu	N	Al
1	850-860	650-690	0,20	0,15	0,41	0,032	0,013	0,15	0,003	0,25	0,004	0,037
2	850-890	650-690	0,18	0,21	0,41	0,038	0,015	0,24	0,002	0,24	0,005	0,039
3	850-870	650-730	0,20	0,27	0,56	0,049	0,018	0,16	0,003	0,25	0,007	0,061
4	850-890	650-690	0,18	0,24	0,47	0,037	0,020	0,17	0,003	0,23	0,004	0,043
5	850-890	650-690	0,14	0,16	0,45	0,041	0,019	0,19	0,002	0,24	0,006	0,043
6	850-890	700-740	0,17	0,15	0,50	0,046	0,010	0,21	0,003	0,24	0,004	0,046
7	850-890	700-740	0,22	0,28	0,60	0,048	0,023	0,21	0,002	0,24	0,005	0,036
8	850-870	700-740	0,21	0,17	0,52	0,049	0,014	0,18	0,002	0,24	0,005	0,041
9	850-890	700-740	0,22	0,15	0,41	0,036	0,014	0,24	0,003	0,24	0,004	0,038
10	850-890	700-740	0,15	0,24	0,60	0,039	0,019	0,21	0,004	0,24	0,005	0,043
11	810-850	550-600	0,22	0,22	0,56	0,042	0,011	0,22	0,007	0,25	0,004	0,036
12	810-850	550-600	0,19	0,21	0,47	0,046	0,009	0,19	0,004	0,26	0,007	0,038
13	810-850	580-520	0,18	0,22	0,47	0,023	0,012	0,16	0,003	0,26	0,005	0,036
14	840-850	600-630	0,14	0,24	0,41	0,036	0,015	0,21	0,006	0,25	0,006	0,046
15	810-850	550-600	0,15	0,15	0,40	0,035	0,016	0,19	0,002	0,24	0,005	0,037
16	810-850	550-600	0,21	0,25	0,57	0,043	0,019	0,26	0,005	0,26	0,005	0,047
17	810-850	550-600	0,16	0,15	0,53	0,035	0,014	0,23	0,008	0,25	0,005	0,035
18	810-850	550-600	0,20	0,21	0,56	0,037	0,009	0,21	0,004	0,28	0,004	0,041

**Table 2: Geometrical dimensions of the sample cover the tensile and mechanical properties of ST3SP**

Melt number	Sample width <i>d</i> , mm		Sample depth <i>t</i> , mm	Sample length <i>l</i> , mm	Yield stress, $\sigma_y$ , MPa		Strength limit, $\sigma_t$ , MPa	
282779	7.55	7.85	4.01	152.7	235.29	241.83	425.21	419.92
192906	7.46	7.86	3.99	152.7	208.37	218.51	388.63	367.39
283444	7.38	7.92	4.09	152.7	234.74	229.19	449.63	462.55
183127	7.29	7.61	4.01	152.7	219.54	216.85	427.82	423.93
313128	7.92	7.41	4.09	152.7	204.83	205.72	378.34	365.81
273373	8.03	8.21	4.09	152.7	216.95	215.85	393.28	396.43
163961	7.62	7.61	4.01	152.7	251.46	244.27	479.29	481.38
253369	7.49	7.82	4.02	152.7	246.65	238.31	433.27	431.76
283397	7.47	7.71	3.97	152.7	214.49	214.84	435.35	411.76
199149	7.61	7.92	3.98	152.7	221.51	219.21	389.47	384.54
223883	7.47	7.49	4.03	152.7	239.28	238.19	395.35	386.76
272884	7.48	7.59	4.01	152.7	241.71	235.23	381.32	382.58
243785	7.84	7.98	4.01	152.7	209.19	204.21	372.54	381.29
216894	7.73	7.82	3.98	152.7	198.92	194.14	363.36	352.76
234647	7.91	7.84	4.01	152.7	204.29	201.83	455.93	471.68
274827	7.48	7.63	4.03	152.7	243.17	239.54	478.32	479.14
283617	7.61	7.29	4.02	152.7	218.41	214.76	392.64	418.27
284731	7.72	7.63	4.09	152.7	265.17	267.93	373.74	374.61

The derived equations are following:

$$\sigma_t = 722.48 [C] + 64.88 [Mn] + 276, 12 [Si] + 201.36 \quad \dots(1)$$

$$\sigma_y = 384.32 [C] + 34.51 [Mn] + 146, 88 [Si] + 97.11 \quad \dots(2)$$

where  $\sigma_t$  and  $\sigma_y$  – tensile strength and yield strength of sheets;

[C], [Mn], [Si] – the content of carbon, manganese and silicon.

The correlation coefficients for equations (1) and (2) were 0.89 and 0.86, respectively.

In case of carbon content fluctuation from 0.14 to 0.22%, manganese content fluctuation from 0.4 to 0.6%, silicon content fluctuation from 0.15 to 0.28% the value of tensile strength and yield strength were found, respectively:

- from 370 to 480 MPa;
- from 196 to 247 MPa.

The results of the analysis allow to conclude that the control of mechanical properties by changing the chemical composition is possible only by setting a sufficiently narrow band of fluctuation of the carbon, manganese and silicon content.

The study of the steel ST3SP structure on an optical microscope «Axiovert-200 MAT» and electron probe microanalyzer JEOL showed that increasing the content of carbon simultaneously leads to increasing the amount of pearlite in ferrite-pearlite structure of the steel is increased (Figs. 2 and 3). In this case, investigated sheet steel has a typical structure consisting of ferrite grains (bright sections) with dimensions of 15-34  $\mu\text{m}$  and sections of lamellar pearlite (dark sections) with dimensions of 18-36  $\mu\text{m}$ , which occupies 55,774-73.443% of the grinding surface. There are rounded carbide particles with dimensions of 0.15-0.07  $\mu\text{m}$  in the volume of ferrite grains and at their boundaries (Fig. 4).

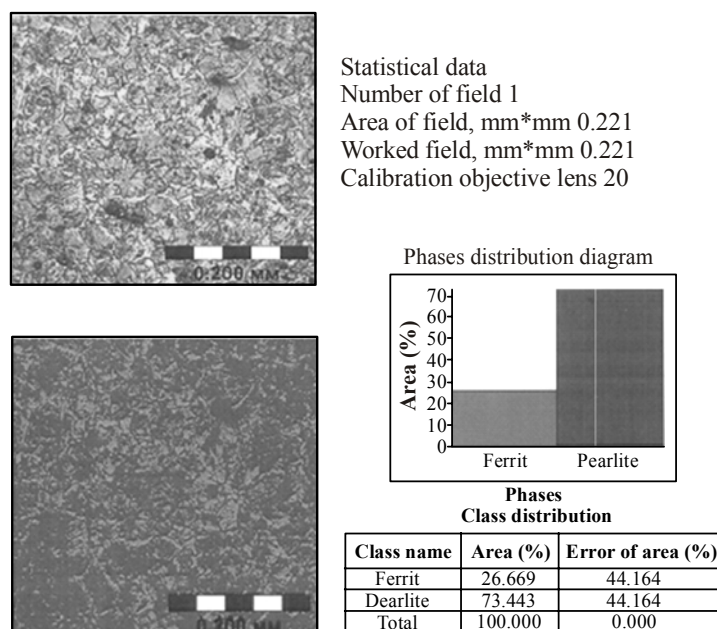


**Fig. 2: Microstructure and distribution diagram in phases of ST3SP steel with a carbon content of 0.22%**

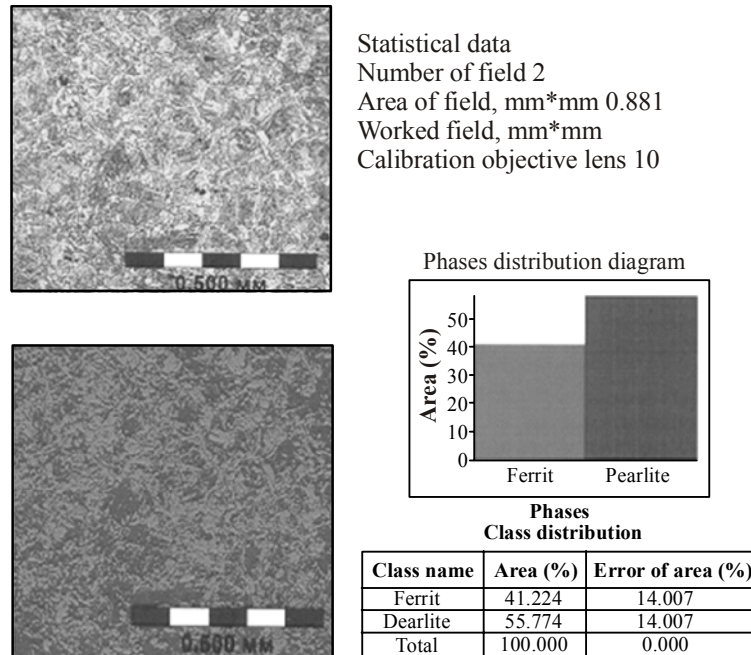


**Fig. 3: Microstructure and distribution diagram in phases of steel ST3SP with a carbon content of 0.14%**

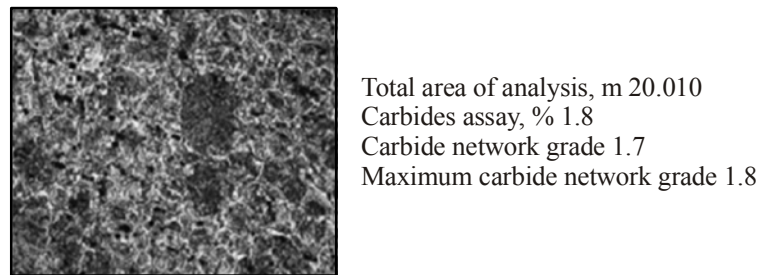


**Fig. 4: The microstructure and the content of carbides in steel ST3SP with a carbon content 0.22%**

The average thickness of the plates of cementite in pearlite areas is 0.1-0.15  $\mu\text{m}$ , and the inter lamellar distance is 0.18-0.27  $\mu\text{m}$ .

It should be noted that small quantities of stretched stringers of manganese sulfide (MnS), aluminum oxide ( $\text{Al}_2\text{O}_3$ ), silica ( $\text{SiO}_2$ ) and nitrides ( $\text{Fe}_4\text{N}$ ) were found in the structure of the studied steel.

Fractographic studies have shown that the fractures of the majority of samples tested have pitted structure, which is indicative for ductile fracture (Fig. 5a). Relatively small fraction surface is cheated by large holes more than 8  $\mu\text{m}$ , in which large particles are appeared, that may include non-metallic particles and carbides in soluble or isolated during heating of the slab, rolling, controlled cooling and coiling hot-rolled strip (Fig. 5a). Most of the fractured surface is covered with pits with sizes of less than 6  $\mu\text{m}$ , in which existents of the particles can also be observed. According to the data obtained it can be concluded that the ductile fracture process is controlled by nucleation and coalescence of micropores<sup>3</sup>.

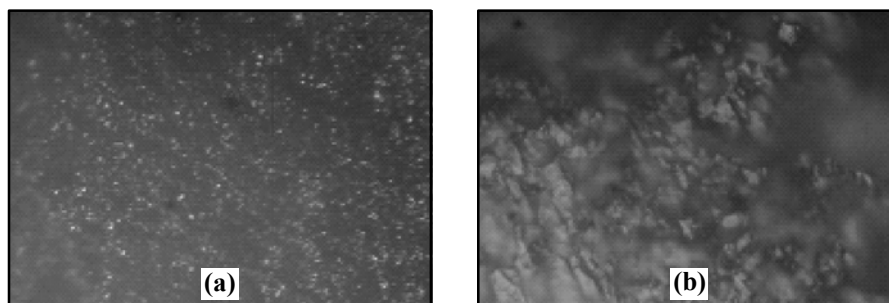


**Fig. 5: The microscopic picture of the steel ST3SP fracture with carbon content of (a) 0.14% and (b) 0.22%**

According to the results of fractographic study it has been found that under the standard tension testing conditions, the destruction of some samples of steel ST3SP is developed by the mechanism of trans granular cleavage (Fig. 5b). In this case, multiple particles of carbides and oxides, which are preferably arranged on the lines of cleavage, are visible. This indicates brittleness of generated particles, leading to nucleation of cracks along their body, which further extend to the whole cross section of the sample. Morphology and number of particles count on fracture surface almost depends on the chemical composition of the investigated steel. It should be borne in mind that at the fracture position of the working part of the sample is sufficiently random and there can be some fluctuations of carbides, oxides, manganese sulphide in a given section of the sample.

The tests results of samples showed that the amount of brittle fracture increases with the grain sizes from 20 to 40  $\mu\text{m}$ . It should be noted that the development of new technological processes of rolling to increase the ductility of the steel should focus on reducing the size of primary particle sizes up to a maximum of 16...25  $\mu\text{m}$ .

Thus, the phenomenon of embrittlement can be caused by three reasons. The first reason is associated with an increase of grain size. The second one is associated with the release of carbide cementite type due to the high temperature of rolling, the wrong



assignment of cooling mode on run-out table and the time of cooling of the metal coils. After a fairly long exposures coagulation carbide phase at the grain boundaries can pass in steel, which may contribute to the appearance of inter granular fracture sites. The third reason is caused by the possible segregation of impurities at the grain boundaries.

### **CONCLUSION**

- (i) Control of the hardness of hot rolled strip by changing its chemical composition is only possible through the establishment of a sufficiently accurate for the content of carbon in manganese and silicon, and strictly observe the temperature of rolling and cooling on run-out table as well as coiling.
- (ii) Fractographic studies of the samples fracture showed that the fracture of most hot-rolled strips has sticky intra granular cellular character.
- (iii) The maximum proportion of brittle inter granular component in this particular section of the test samples increases with the concentration of carbides, oxides, manganese sulfide.
- (iv) Grinding grain structure and reducing the concentration of impurities improves ductility of the steel ST3SP.

### **REFERENCES**

1. S. A. Mashekov, I. I. Kuzminov and L. A. Kurmangaliev, *Technology of Rolling Production*, Almaty: Teraprint (2007) p. 334.
2. M. E. Drita and M. A. Maskalev, *Technology of Structured Materials and Materials Science*, M.: High Scholl (1990) p. 447.
3. K. H. Schwalbe, *Einfluss der Gefügestruktur auf das Bruchverhalten Metallischer Werkstoffe aus der Sicht der Bruchmechanik, Gefüge und Bruch*. Berlin-Stuttgart, 38-43 (1977).

*Accepted : 14.08.2013*